

# Synthesis and Spectroscopic and Electrochemical Properties of TTF-Derivatized Polycarbazole

Yibo Liu,<sup>†</sup> Chengyun Wang,<sup>\*,†</sup> Meijiang Li,<sup>‡</sup> Guoqiao Lai,<sup>‡</sup> and Yongjia Shen<sup>\*,†</sup>

Laboratory of Advanced Materials and Institute of Fine Chemicals, East China University of Science & Technology, Shanghai 200237, P. R. China, and Key Lab of Organosilicon Chemistry and Material Technology of Ministry of Education, Hangzhou Normal University, Hangzhou 310012, P. R. China

Received September 8, 2007; Revised Manuscript Received January 11, 2008

**ABSTRACT:** Two polycarbazoles with tetrathiafulvalene (TTF) as pendant group were synthesized first by Yamamoto coupling reaction using Ni(1,5-cyclooctadiene)<sub>2</sub> (Ni(COD)<sub>2</sub>) as the catalyst. The structures of the polymers and their intermediates were characterized by <sup>1</sup>H NMR, <sup>13</sup>C NMR, MS, GPC, UV–vis, and IR. The electrochemical behaviors of the polymers were characterized by cyclic voltammetry. These polymers exhibit higher conductivity up to about 0.1 S cm<sup>-1</sup>.

## Introduction

Carbazole-containing polymers, especially the carbazole-based conjugated copolymers and homopolymers, have been extensively investigated as light-emitting materials, photorefractive materials, hole-transporting, photoconductors, and conducting materials, based on their hole transport ability and electrochemical and spectroscopic properties.<sup>1–6</sup>

Tetrathiafulvalene (TTF) and its derivatives are also of interesting because they possess unique electron-donating properties and can form conducting charge-transfer complexes (CT complexes). Especially, the crystals of TTF-based CT complexes possess metallic conductivity because of the regular formation of segregated stacks of donors and acceptors and a certain degree of charge transfer between the stacks. Despite the inherent electronic advantages, the crystals of TTF-based CT complexes tend to be brittle and unprocessable, which is a major obstacle to practical applications. In order to overcome the problem, there have been several attempts to incorporate TTF into polymeric matrixes. Several research groups have made some work to design and synthesize polymeric TTFs.<sup>7–9</sup> Some  $\pi$ -conjugated polymers containing TTF moieties have been successfully synthesized as well.<sup>10–13</sup> Such an approach is based on the following points: (1) From the conjugated polymers viewpoint, the propensity of TTF to form ordered stacks can represent an interesting tool to control the long-range order of the conjugated backbone. (2) In the frame of TTF-based conductors, such a combination can contribute to an increase in the dimensionality of the conducting process and the processability of TTF-based conductors. Furthermore, the grafting of TTF groups on conjugated polymer's backbone may lead to a significant increase of the charge storage capacity of the resulting substituted conjugated polymer.

In this paper, we present the synthesis of two TTF-derivatized polycarbazoles. To our knowledge, it may be the first example, in which TTF had been attached as pendant groups to polycarbazole.

## Results and Discussion

**Synthesis.** Scheme 1 describes the synthetic procedure of **2**, **4**, and **5**. 1-(2-Cyanoethylthio)-2,3,4-trimethylthio-TTF (**3**) was

\* Corresponding authors. Y.S.: Tel +86 021 64252967; e-mail yjshen@ecust.edu.cn. C.W.: Fax +86 021 64252967; e-mail cywang@ecust.edu.cn.

<sup>†</sup> East China University of Science & Technology.

<sup>‡</sup> Hangzhou Normal University.

Table 1. GPC Data of **5a** and **5b**

polymer	<i>M<sub>n</sub></i>	<i>M<sub>w</sub></i>	<i>M<sub>w</sub>/M<sub>n</sub></i>
<b>5a</b>	33 285	58 249	1.75
<b>5b</b>	36 889	59 761	1.62

Table 2. UV–Vis Absorption and Oxidative Potentials of **5a**, **5b**, **4a**, and **4b** in CH<sub>2</sub>Cl<sub>2</sub>

compound	UV–vis $\lambda_{\text{max}}$ (nm)	CV ( <i>E</i> <sub>1/2</sub> /V)
<b>4a</b>	335	0.57, 0.87, 1.29
<b>5a</b>	318	0.67, 1.04
<b>4b</b>	335	0.57, 0.87, 1.30
<b>5b</b>	319	0.66, 1.05

synthesized according to the literature.<sup>14</sup> Carbazole reacted with bromine in a mixture of carbon disulfide and pyridine solution to give 3,6-dibromocarbazole (**1**) in 83% yield. N-alkylation of the nitrogen atom in 3,6-dibromocarbazole with 1,3-dibromopropane or 1,5-dibromopentane in the presence of KOH afforded *N*-3-bromopropanyl-3,6-dibromocarbazole (**2a**) and *N*-5-bromopentanyl-3,6-dibromocarbazole (**2b**), respectively. Deprotection of 2-cyanoethyl groups in **3** with the aid of CsOH monohydrate and sequentially reaction with **2a** or **2b** afforded **4a** or **4b**, after purification with column chromatography. Homopolymer **5a** or **5b** was obtained by the Yamamoto coupling reaction<sup>15</sup> of **4a** or **4b** using Ni(COD)<sub>2</sub> as the catalysts. The GPC indicated the distribution of average molecular weight of **5a** and **5b**, which is shown in Table 1. **5a** and **5b** were reasonably soluble in common organic solvents, such as chloroform, THF, toluene, dichloromethane, and 1,2-dichloroethane. They also showed good film-forming ability, which made them easily fabricated into thin film using either spin-coating or solvent-casting techniques.

**UV–Vis Spectra and Cyclic Voltammetry.** The maximum UV–vis absorption and oxidative potentials of **4a**, **4b**, **5a**, and **5b** in CH<sub>2</sub>Cl<sub>2</sub> are listed in Table 2. The UV–vis spectra and cyclic voltammogram of the polymer **5a** and monomer **4a**, which were similar to those of **5b** and **4b**, for examples, are shown in Figures 1 and 2.

Figure 1 shows the UV–vis spectra of **5a** and **4a** in CH<sub>2</sub>Cl<sub>2</sub>. **4a** exhibited two maximum absorptions at 315 and 334 nm and a wide absorption in the range between 360 and 445 nm. **5a** exhibited a wide absorption in the range between 300 and 330 nm and a maximum absorption at 318 nm; it was close to the absorption of polycarbazole (300–320 nm).<sup>16</sup> Obviously, a wide absorption in the range between 360 and 445 nm belongs to the TTF moiety in the polymer.

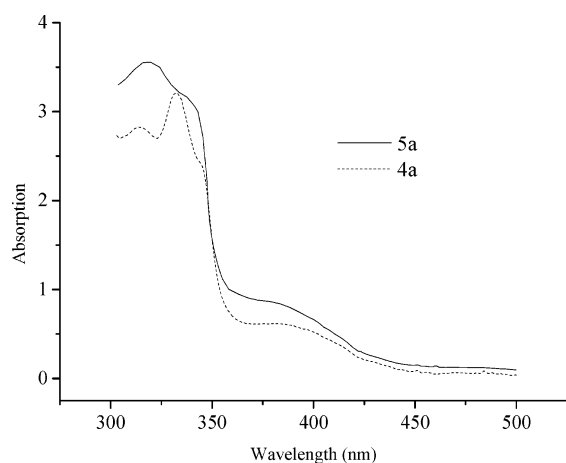
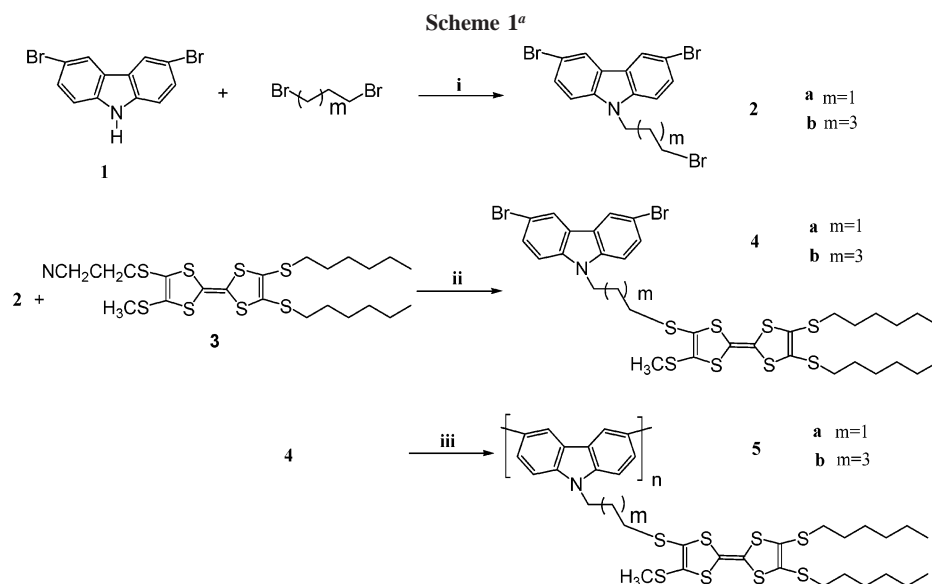


**Figure 1.** UV-vis spectra of **5a** and **4a** in CH<sub>2</sub>Cl<sub>2</sub>.

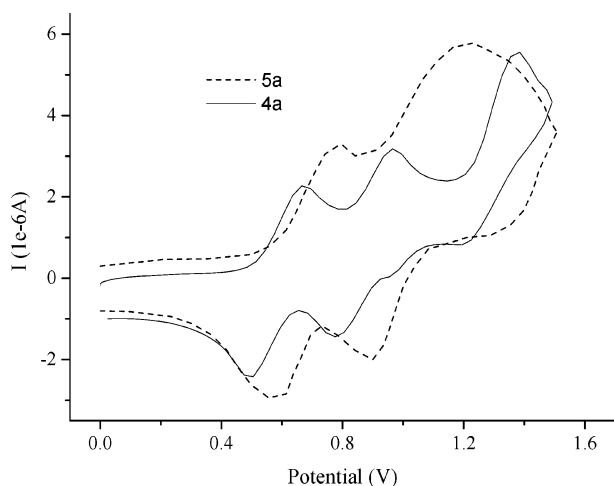


**Figure 2.** Cyclic voltammogram of **5a** and **4a** in CH<sub>2</sub>Cl<sub>2</sub>.

The redox behaviors of **4a**, **4b** and their homopolymer **5a**, **5b** in CH<sub>2</sub>Cl<sub>2</sub> were measured by cyclic voltammetry with *n*-Bu<sub>4</sub>-NPF<sub>6</sub> as the supporting electrolyte, platinum as the working and counter electrodes, and Ag/AgCl as the reference electrode; the scan rate was 100 mV/s, as shown in Figure 2 and Table 2. **4a** showed three one-electron quasi-reversible oxidation potentials at 0.57, 0.87, and 1.29 V, corresponding to the radical cation

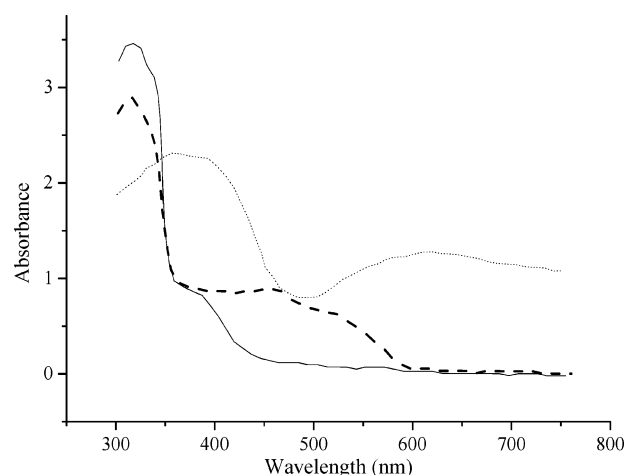


**Figure 3.** UV-vis spectroelectrochemistry of **5a** on quartz (—), at 0.7 V on ITO (---), and 1.2 V on ITO glass (···) in acetonitrile.

TTF<sup>+</sup>, dication TTF<sup>2+</sup>, and free cation of carbazole, respectively. The cathode wave of carbazole<sup>+</sup> was small and un conspicuous. Interestingly, **5a** showed first one-electron reversible oxidation wave at 0.67 V, which was substantially higher than the corresponding values of **4a**. This phenomenon probably indicated that the oxidation of TTF moiety was influenced by polycarbazole moiety. The second oxidation potential of **5a** was at 1.04 V. Its anodic wave was higher and wider compared to that of **4a**, and seemed as a overlap of waves, which might be overlapped from the second anodic wave of TTF dication moiety and the anodic wave of polycarbazole moiety (0.9 V).<sup>17</sup>

**UV-Vis Spectroelectrochemistry.** UV-vis spectroelectrochemistry on ITO glass **5a** and **5b** in acetonitrile upon oxidation is shown in Figure 3. The spectra of **5a**, similar to that of **5b**, showed very evident change in the band corresponding to the absorption wavelength of the neutral polymer. The wide wavelength absorption band from 400 to 600 nm at 0.7 V was probably due to the absorption of the TTF<sup>+</sup> (430 and 580 nm).<sup>18</sup> At 1.2 V, the initial band around the 400 nm might be probably due to the absorption of the TTF<sup>2+</sup>. Polycarbazole moiety in polymers gave rise to the absorption band at 550 nm, similar to that of the *N*-alkylpolycarbazole;<sup>19</sup> in addition, the other absorption band of the TTF<sup>2+</sup> (600 nm) was inconspicuous and

**Table 3.** Conductivity of **5a**, **5b**, and *N*-Alkylpolycarbazole

polymer	in-situ conductivity (S cm <sup>-1</sup> )	ex-situ conductivity (S cm <sup>-1</sup> )
<b>5a</b>	$9 \times 10^{-2}$	$1 \times 10^{-1}$
<b>5b</b>	$8 \times 10^{-2}$	$1 \times 10^{-1}$
<i>N</i> -alkylpolycarbazole	$10^{-3}$ – $10^{-4}$	$10^{-3}$ – $10^{-4}$ <sup>a</sup>

<sup>a</sup> Doped by I<sub>2</sub>.<sup>19</sup>

perhaps hidden underneath the largely absorption band for the polycarbazole.

**Conductivity.** Table 3 shows the conductivities of **5a** and **5b**, measured by an electrochemical technique (in situ conductivity) and after chemical oxidation with TCNQ (ex-situ conductivity), together with *N*-alkylpolycarbazole.<sup>19</sup>

In-situ conductivity measurements of the polymers represent the highest conductivity obtained for the polymer as a film on an electrode and show that oxidation cause the transition from an insulating to a conductive state as generally found in polyconjugated polymer.

The conductivity of the polymers as a function of the applied potential displays a sigmoid shape (see Figure 4). The conductivity of **5a** and **5b** was about  $10^{-5}$  S cm<sup>-1</sup> at lower potential. At the potential 0.7 V, the TTF moiety of the polymer was oxidized to TTF<sup>+</sup>, which facilitated the  $\pi$ – $\pi$  interaction between neighboring TTF units (intra- and intermolecular reactions) just as other conducting TTF-based polymers.<sup>20</sup> When the potential applied was increased from the first potential (0.7 V) to the second one (1.2 V), the conductivity was increased fiercely and reached a maximal plateau ( $9 \times 10^{-2}$  and  $8 \times 10^{-2}$  S cm<sup>-1</sup>, respectively). In this process, polycarbazole moiety in the polymers were oxidized, the highly delocalized charges between the TTF and conjugated polycarbazole backbone aroused the higher conductivity. On the other hand, the higher conductivity probably benefited also from the redox charge transport, which was composed of the electron transport within the polycarbazole moiety and the electron hopping within the TTF moiety.

In ex-situ conductivity measurements, the solution of the polymer in THF was treated with varying volumes of the electron acceptor tetracyanoquinodimethane (TCNQ), and the subsequent polymer films were prepared by spin-coating its CH<sub>2</sub>-Cl<sub>2</sub> solution onto ITO glass plate, followed by drying in vacuum at 30 °C for 5 h. The electric conductivity of the TCNQ-doped polymer was measured using a four-probe technique with a SZ85 apparatus. The maximum conductivity observed in the doped films was 0.1 S cm<sup>-1</sup>, which derived from a 1:2 molar mixture of polymer/TCNQ. On the other hand, the doped

polymers were stable in air; their conductivities were almost changeless just like other TTF-based polymers. Compared to the in-situ conductivity, the slightly higher ex-situ conductivity of polymers **5a** and **5b** could be related to the presence of branched substituents, which were necessary to allow the solubilization of the deposited polymer.

Both **5a** and **5b** possess higher conductivity than most of polycarbazole and other TTF-based polymers performed by an electrochemical doping (in-situ conductivity) and chemical oxidation doping with TCNQ (ex-situ conductivity). This interesting result is based on two points. From the polycarbazole viewpoint, conjugation backbone will participate and facilitate the mobilization of the charges along the polycarbazole backbone and hence cause an increase in the conductivity. On the other hand, TTF is known to form charge-transfer (CT) complexes with an electron acceptor; in the frame of TTF-based conductors, such a combination can contribute to increase the charges and the dimensionality of the conduction process. So this combination might eventually lead to materials presenting hybrid conduction.

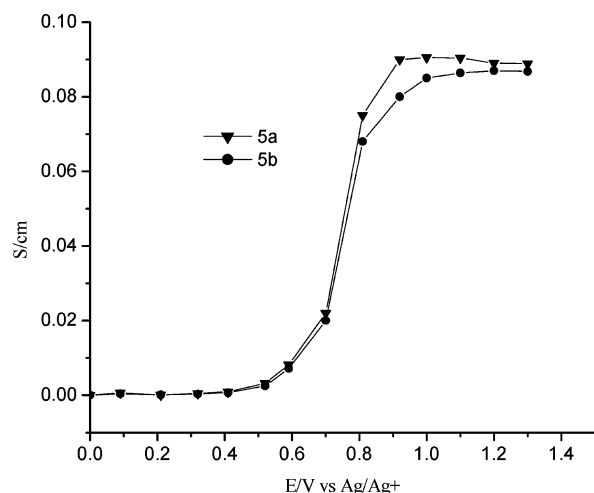
## Conclusion

Two TTF-derivatized polycarbazoles were synthesized by the Yamamoto coupling reaction in the presence of Ni(COD)<sub>2</sub>/COD/2,2'-bipy, whose *M<sub>n</sub>* was 33 285 and 36 889, respectively. These two polymers exhibited higher conductivity up to about 0.1 S cm<sup>-1</sup> performed by an electrochemical doping (in-situ conductivity) and chemical oxidation doping with TCNQ (ex-situ conductivity).

## Experiments

All the reagents and solvents were of commercial quality and were distilled or dried where necessary using the standard procedures. <sup>1</sup>H NMR spectra were recorded on Bruker 400 instrument. Mass spectra were recorded using LCQ ADVANTAGE mass spectrometer. Elemental analyses were performed on Vario EL III. Gel permeation chromatography (GPC) was carried out using toluene as a solvent. Thermogravimetric analysis was performed on a MOM Paulik-pauli-Erdey derivatograph at a 10 °C /min heating rate, in air. Absorption spectra were measured with Nicolet evolution 300 UV–vis spectrophotometer. Electrochemical experiments were performed with IM6e at 25 °C under nitrogen in three electrode cells. The counter and working electrode was platinum; the reference electrode was Ag/Ag<sup>+</sup> (–0.04 V vs SCE). The voltammetric apparatus included a PGSTAT30 potentiostat modulated by a programmable function generator and coupled to a digital integrator. Spectroelectrochemical spectra were obtained from a Perkin-Elmer Lambda 15 spectrometer. A 0.8 × 2.5 cm indium–tin oxide (ITO) sheet was used. *n*-Bu<sub>4</sub>NPF<sub>6</sub> was used as the supporting electrolyte. The apparatus and procedures used for the in-situ conductivity experiments were actualized according to the literature.<sup>21</sup> The electrode for conductivity measurements was typically a two-band platinum spacing of 20 μm. In the case of conductivities lower than 10<sup>-2</sup> S cm<sup>-1</sup>, the electrode was a microband array platinum electrode (5 μm bandwidth, 100 nm thick) with interband spacing of 5 μm. The deposit was thick enough to ensure minimum resistance, under which condition the conductivity  $\sigma$  is given by  $\sigma = k/(R - R_0)$ , where *R* is the measured resistance, *R*<sub>0</sub> is the lead resistance, and *k* is the cell constant.

**Synthesis of 2a.** To a solution of **1** (2 g, 6.2 mmol) in dried DMF (30 mL) was added KOH powder (4 g, 0.1 mol). The mixture was stirred for 3 h and then added dropwise slowly into 1,3-dibromopropane (10 g, 50 mmol). The solution was stirred overnight and then poured into water and extracted with chloroform three times. The combined organic layer was dried over anhydrous magnesium sulfate. After removing the solvent and unreacted 1,3-dibromopropane in vacuo, the residue was crystallized in methanol

**Figure 4.** In-situ conductivity for **5a** and **5b**.



twice to afford **2a** as white crystal (1.76 g, yield 64%).  $^1\text{H}$  NMR ( $\text{CDCl}_3$ , 400 MHz):  $\delta$  7.87 (s, 2H, Ph-H), 7.62 (d, 2H,  $J = 4$  Hz, Ph-H), 7.35 (d, 2H,  $J = 4$  Hz, Ph-H), 4.41 (t, 2H,  $J = 8$  Hz, N-CH<sub>2</sub>-), 3.38 (t, 2H,  $J = 8$  Hz, -CH<sub>2</sub>-Br), 2.41 (m, 2H, -CH<sub>2</sub>-). ESI MS  $m/z$ : 443.65 ( $M^+$ ). Anal. Calcd for  $\text{C}_{15}\text{H}_{12}\text{NBr}_3$ : C, 40.40; H, 2.71; N, 3.14. Found: C, 40.39; H, 2.73; N, 3.15. IR (KBr):  $\nu$ ,  $\text{cm}^{-1}$ , 1590, 1487, 1038.

**Synthesis of 2b.** **2b** was synthesized by the same procedure above, just using 1,5-dibromopentane instead of 1,3-dibromopropane; yield 61%.  $^1\text{H}$  NMR ( $\text{CDCl}_3$ , 400 MHz):  $\delta$  7.87 (s, 2H, Ph-H), 7.62 (d, 2H,  $J = 4$  Hz, Ph-H), 7.35 (d, 2H,  $J = 4$  Hz, Ph-H), 4.41 (t, 2H,  $J = 8$  Hz, N-CH<sub>2</sub>-), 3.38 (t, 2H,  $J = 8$  Hz, -CH<sub>2</sub>-Br), 1.79 (m, 2H,  $J = 8$  Hz, -CH<sub>2</sub>-), 1.76 (m, 2H, -CH<sub>2</sub>-), 1.28 (m, 2H, -CH<sub>2</sub>-). ESI MS  $m/z$ : 471.05 ( $M^+$ ). Anal. Calcd for  $\text{C}_{17}\text{H}_{16}\text{NBr}_3$ : C, 43.07; H, 3.40; N, 2.95. Found: C, 43.08; H, 3.42; N, 2.94. IR (KBr):  $\nu$ ,  $\text{cm}^{-1}$ , 1591, 1487, 1038.

**Synthesis of 4a.** To a solution of **3** (1 g, 1.8 mmol) in dried DMF (30 mL) was added a solution of  $\text{CsOH}\cdot\text{H}_2\text{O}$  (355 mg, 2.1 mmol) in dried MeOH (5 mL) over a period of 30 min. The mixture was stirred for an additional 30 min and then added dropwise to a solution of **2a** (823 mg, 1.8 mmol) in dried DMF (20 mL) for 2 h. The solution was stirred overnight. After removing solvents under reduced pressure and separation by column chromatography on silica gel with  $\text{CH}_2\text{Cl}_2/\text{hexane}$ : (1/8, v/v) as eluent. **4a** was obtained as dark-red solid (663 mg, yield 42%).  $^1\text{H}$  NMR ( $\text{CDCl}_3$ , 400 MHz):  $\delta$  7.86 (s, 2H, Ph-H), 7.62 (d, 2H,  $J = 4$  Hz, Ph-H), 7.35 (d, 2H,  $J = 4$  Hz, Ph-H), 4.40 (t, 2H,  $J = 8$  Hz, N-CH<sub>2</sub>-), 2.81 (t, 6H,  $J = 8$  Hz, S-CH<sub>2</sub>-), 2.48 (s, 3H, S-CH<sub>3</sub>). 2.20 (m, 2H, -CH<sub>2</sub>-), 1.63 (m, 4H, -CH<sub>2</sub>-), 1.58 (m, 4H, -CH<sub>2</sub>-), 1.40 (m, 4H, -CH<sub>2</sub>-), 1.28 (m, 4H, -CH<sub>2</sub>-). 0.89 (t, 6H,  $J = 4$  Hz, -CH<sub>3</sub>).  $^{13}\text{C}$  NMR [ $\text{CDCl}_3$ , 100 MHz]: 140.33, 130.95, 127.86, 125.70, 122.91, 120.42, 118.90, 108.62, 42.55, 36.34, 35.94, 31.32, 29.74, 28.23, 27.36, 19.13, 15.07. ESI MS  $m/z$ : 876.81 ( $M^+$ ). Anal. Calcd for  $\text{C}_{34}\text{H}_{41}\text{NS}_8\text{Br}_2$ : C, 46.40; H, 4.70; N, 1.59. Found: C, 46.39; H, 4.73; N, 1.60. IR (KBr):  $\nu$ ,  $\text{cm}^{-1}$ , 2922, 2854, 1636, 1590, 1487, 1417, 1261, 1038.

**Synthesis of 4b.** **4b** was synthesized by the same procedure above, just using **2b** instead of **2a**; yield 46%.  $^1\text{H}$  NMR ( $\text{CDCl}_3$ , 400 MHz):  $\delta$  7.86 (s, 2H, Ph-H), 7.62 (d, 2H,  $J = 4$  Hz, Ph-H), 7.35 (d, 2H,  $J = 4$  Hz, Ph-H), 4.40 (t, 2H,  $J = 8$  Hz, N-CH<sub>2</sub>-), 2.81 (t, 6H,  $J = 8$  Hz, S-CH<sub>2</sub>-), 2.48 (s, 3H, S-CH<sub>3</sub>). 1.80 (m, 2H, -CH<sub>2</sub>-), 1.78 (m, 2H, -CH<sub>2</sub>-), 1.63 (m, 4H, -CH<sub>2</sub>-), 1.58 (m, 4H, -CH<sub>2</sub>-), 1.40 (m, 4H, -CH<sub>2</sub>-), 1.30 (m, 2H, -CH<sub>2</sub>-), 1.28 (m, 4H, -CH<sub>2</sub>-). 0.89 (t, 6H,  $J = 4$  Hz, -CH<sub>3</sub>).  $^{13}\text{C}$  NMR [ $\text{CDCl}_3$ , 100 MHz]: 140.33, 130.95, 127.86, 125.70, 122.91, 120.42, 118.90, 108.62, 42.55, 36.34, 35.94, 31.32, 30.12, 29.74, 28.23, 27.36, 26.51, 19.13, 15.07. ESI MS  $m/z$ : 905.12 ( $M^+$ ). Anal. Calcd for  $\text{C}_{36}\text{H}_{45}\text{NS}_8\text{Br}_2$ : C, 47.62; H, 4.99; N, 1.54. Found: C, 47.61; H, 4.98; N, 1.55. IR (KBr):  $\nu$ ,  $\text{cm}^{-1}$ , 2923, 2850, 1636, 1590, 1488, 1417, 1262, 1038.

**Synthesis of 5a.** **4a** (877 mg, 1 mmol) was dissolved in dried DMF (10 mL) and added dropwise to a hot solution (50 °C) of  $\text{Ni}(\text{COD})_2$  (359 mg, 1.3 mmol), COD (0.1 mL), and 2,2'-bipy (157 mg, 1.3 mmol) in dried DMF under nitrogen. The reaction was stirred for 24 h at 60 °C under nitrogen. The reaction mixture was poured into ethanol (200 mL) and filtrated, and the precipitate was extracted sequentially with ethanol and chloroform (each for 10 h) using a Soxhlet apparatus. The chloroform fraction was evaporated under reduced pressure. The residue was dissolved in chloroform (5 mL) and added to ethanol (50 mL). The precipitate was collected by filtration to afford the polymer **5a** as a dark-red powder (345 mg, 48%).  $^1\text{H}$  NMR ( $\text{CDCl}_3$ , 400 MHz):  $\delta$  7.87–7.60 (m, 4H, Ph-H), 7.37–7.34 (m, 2H, Ph-H), 4.41–4.39 (m, 2H, N-CH<sub>2</sub>-), 2.84–2.77 (m, 6H, S-CH<sub>2</sub>-), 2.50–2.45 (m, 3H, S-CH<sub>3</sub>),

2.21–2.18 (m, 2H, -CH<sub>2</sub>-), 1.65–1.39 (m, 12H, -CH<sub>2</sub>-), 1.30–1.25 (m, 4H, -CH<sub>2</sub>-), 0.91–0.87 (m, 6H, -CH<sub>3</sub>).  $^{13}\text{C}$  NMR [ $\text{CDCl}_3$ , 100 MHz]: 140.32, 130.93, 127.88, 125.71, 122.90, 120.43, 118.88, 108.62, 42.56, 36.35, 35.92, 31.32, 29.74, 28.21, 27.36, 19.15, 15.06.  $M_n = 33\,285$ ,  $M_w/M_n = 1.75$ , corresponding to  $n = 46$ . Anal. Calcd for  $[\text{C}_{34}\text{H}_{41}\text{NS}_8]_n$ : C, 56.75; H, 5.70; N, 1.95. Found: C, 56.71; H, 5.72; N, 1.98. IR (KBr):  $\nu$ ,  $\text{cm}^{-1}$ , 2922, 2854, 1636, 1590, 1487, 1417, 1261.

**Synthesis of 5b.** **5b** was synthesized by the same procedure above, just using **4b** instead of **4a**; yield 50%.  $^1\text{H}$  NMR ( $\text{CDCl}_3$ , 400 MHz):  $\delta$  7.87–7.60 (m, 4H, Ph-H), 7.37–7.34 (m, 2H, Ph-H), 4.41–4.39 (m, 2H, N-CH<sub>2</sub>-), 2.84–2.77 (m, 6H, S-CH<sub>2</sub>-), 2.50–2.45 (m, 3H, S-CH<sub>3</sub>), 1.81–1.76 (m, 4H, -CH<sub>2</sub>-), 1.65–1.39 (m, 12H, -CH<sub>2</sub>-), 1.30–1.25 (m, 6H, -CH<sub>2</sub>-), 0.91–0.87 (m, 6H, -CH<sub>3</sub>).  $^{13}\text{C}$  NMR [ $\text{CDCl}_3$ , 100 MHz]: 140.35, 130.97, 127.88, 125.72, 122.93, 120.44, 118.90, 108.61, 42.54, 36.33, 35.95, 31.32, 30.10, 29.76, 28.23, 27.37, 26.50, 19.12, 15.06.  $M_n = 36\,889$ ,  $M_w/M_n = 1.62$ , corresponding to  $n = 40$ . Anal. Calcd for  $[\text{C}_{36}\text{H}_{45}\text{NS}_8]_n$ : C, 57.83; H, 6.02; N, 1.87. Found: C, 57.88; H, 5.99; N, 1.84. IR (KBr):  $\nu$ ,  $\text{cm}^{-1}$ , 2922, 2854, 1636, 1592, 1501, 1418, 1261.

**Acknowledgment.** This work was supported by National Natural Science Foundation of China (No. 20676036), Specialized Research Fund for the Doctoral Program of Higher Education (No. 20070251018), and the foundation of East China University of Science & Technology (YJ0142130).

## References and Notes

- (1) Grazulevicius, J. V.; Strohriegel, P.; Pielichowski, J.; Pielichowski, K. *Prog. Polym. Sci.* **2003**, *28*, 1297.
- (2) Morin, J. F.; Leclerc, M.; Adès, D.; Siove, A. *Macromol. Rapid Commun.* **2005**, *26*, 761.
- (3) Maruyama, S.; Tao, X. T.; Hokari, H.; Noh, T.; Zhang, Y.; Wada, T.; Sasabe, H.; Suzuki, H.; Watanabe, T.; Miyata, S. *J. Mater. Chem.* **1999**, *9*, 893.
- (4) Sasabe, H.; Zhang, Y.; Wada, T.; Wang, L. *Chem. Mater.* **1997**, *9*, 2798.
- (5) Thomas, K. R. J.; Lin, J. T.; Tao, Y. T.; Ko, C. W. *J. Am. Chem. Soc.* **2001**, *123*, 9404.
- (6) Hwang, J.; Sohn, J.; Park, S. Y. *Macromolecules* **2003**, *36*, 7970.
- (7) Charles, U.; Pittman, J.; Ueda, M.; Liang, F. Y. *J. Org. Chem.* **1979**, *44*, 3639.
- (8) Ueno, Y.; Masuyama, Y.; Okawara, M. *Chem. Lett.* **1975**, 603.
- (9) Frenzel, S.; Baumgarten, M.; Müllen, K. *Synth. Met.* **2001**, *118*, 97.
- (10) Thobie-Gautier, C.; Gorgues, A.; Jubault, M.; Roncali, J. *Macromolecules* **1993**, *26*, 4094.
- (11) Huchet, L.; Akoudad, S.; Roncali, J. *Adv. Mater.* **1998**, *10*, 541.
- (12) Charlton, A.; Underhill, A. E.; Williams, G.; Kalaji, M.; Murphy, P. J.; Hibbs, D. E.; Hursthouse, M. B.; Abdul, Malik, K. M. *Chem. Commun.* **1996**, 2423.
- (13) Bryce, M. R.; Chissel, A. D.; Gopal, J.; Kathirgamanathan, P.; Parker, D. *Synth. Met.* **1991**, *39*, 397.
- (14) Simonsen, K. B.; Svenstrup, N.; Lau, J.; Simonsen, O.; Kristensen, G. J.; Becher, J. *Synthesis* **1996**, 407.
- (15) Zhang, Z. B.; Fujiki, M.; Tang, H. Z.; Motonaga, M.; Torimitsu, K. *Macromolecules* **2002**, *35*, 1988.
- (16) Siove, A.; Adès, D.; Chevrot, C.; Froyer, G. *Makromol. Chem.* **1989**, *190*, 1361.
- (17) Macit, H.; Sen, S.; Sacak, M. *J. Appl. Polym. Sci.* **2005**, *96*, 894.
- (18) Spanggaard, H.; Prehn, J.; Nielsen, M. B.; Levillain, E.; Allain, M.; Becher, J. *J. Am. Chem. Soc.* **2000**, *122*, 9486.
- (19) Zotti, G.; Schiavon, G.; Zecchin, S.; Morin, J. F.; Leclerc, M. *Macromolecules* **2002**, *35*, 2111.
- (20) Frenzel, S.; Arndt, S.; Ma, R.; Müllen, K. *J. Mater. Chem.* **1995**, *10*, 1529.
- (21) Aubert, P. H.; Groenecdaal, L.; Louwet, F.; Lutsen, L.; Vanderzande, D.; Zotti, G. *Synth. Met.* **2002**, *126*, 193.

MA702035C